

**Sun and volcanoes:
effect on the
troposphere in the
DM**

J. G. Anet et al.

Impact of solar vs. volcanic activity variations on tropospheric temperatures and precipitation during the Dalton Minimum

J. G. Anet¹, S. Muthers^{2,3}, E. V. Rozanov^{1,4}, C. C. Raible^{2,3}, A. Stenke¹,
A. I. Shapiro⁴, S. Brönnimann^{5,3}, F. Arfeuille^{5,3}, Y. Brugnara^{5,3}, J. Beer⁶,
F. Steinhilber⁶, W. Schmutz⁴, and T. Peter¹

¹Institute for Atmospheric and Climate Science ETH, Zurich, Switzerland

²Climate and Environment Physics, Physics Institute, University of Bern, Bern, Switzerland

³Oeschger Centre for Climate Change Research, University of Bern, Bern, Switzerland

⁴Physikalisch-Meteorologisches Observatorium Davos and World Radiation Center (PMOD/WRC), Davos, Switzerland

⁵Institute of Geography, University of Bern, Bern, Switzerland

⁶Eawag, Surface Waters group, Kastanienbaum, Switzerland

[Title Page](#)

[Abstract](#)

[Introduction](#)

[Conclusions](#)

[References](#)

[Tables](#)

[Figures](#)

[⏪](#)

[⏩](#)

[◀](#)

[▶](#)

[Back](#)

[Close](#)

[Full Screen / Esc](#)

[Printer-friendly Version](#)

[Interactive Discussion](#)

Received: 21 October 2013 – Accepted: 26 October 2013 – Published: 4 November 2013

Correspondence to: J. G. Anet (julien.anet@alumni.ethz.ch) and E. Rozanov (eugene.rozanov@pmodwrc.ch)

Published by Copernicus Publications on behalf of the European Geosciences Union.

CPD

9, 6179–6220, 2013

**Sun and volcanoes:
effect on the
troposphere in the
DM**

J. G. Anet et al.

Title Page

Abstract

Introduction

Conclusions

References

Tables

Figures



Back

Close

Full Screen / Esc

Printer-friendly Version

Interactive Discussion



Abstract

The aim of this work is to elucidate the impact of changes in solar irradiance and energetic particles vs. volcanic eruptions on tropospheric global climate during the Dalton Minimum (DM, 1780–1840 AD). Separate variations in the (i) solar irradiance in the UV-C with wavelengths $\lambda < 250$ nm, (ii) irradiance at wavelengths $\lambda > 250$ nm, (iii) in energetic particle spectrum, and (iv) volcanic aerosol forcing were analyzed separately, and (v) in combination, by means of small ensemble calculations using a coupled atmosphere-ocean chemistry-climate-model. Global and hemispheric mean surface temperatures show a significant dependence on solar irradiance at $\lambda > 250$ nm. Also, powerful volcanic eruptions in 1809, 1815, 1831 and 1835 significantly decrease global mean temperature by up to 0.5 K for 2–3 yr after the eruption. However, while the volcanic effect is clearly discernible in the southern hemispheric mean temperature, it is less significant in the Northern Hemisphere, partly because the two largest volcanic eruptions occurred in the SH tropics and during seasons when the aerosols were mainly transported southward, partly because of the higher northern internal variability. In the simulation including all forcings, temperatures are in reasonable agreement with the tree-ring-based temperature anomalies of the Northern Hemisphere. Interestingly, the model suggests that solar irradiance changes at $\lambda < 250$ nm and in energetic particle spectra have only insignificant impact on the climate during the Dalton Minimum. This downscapes the importance of top-down processes (stemming from changes at $\lambda < 250$ nm) relative to bottom-up processes (from $\lambda > 250$ nm). Reduction of irradiance at $\lambda > 250$ nm leads to a significant (up to 2 %) decrease of the ocean heat content (OHC) between the 0 and 300 m of depth, whereas the changes in irradiance at $\lambda < 250$ nm or in energetic particle have virtually no effect. Also, volcanic aerosol yields a very strong response, reducing the OHC of the upper ocean by up to 1.5 %. In the simulation with all forcings, the OHC of the uppermost levels recovers after 8–15 yr after volcanic eruption, while the solar signal and the different volcanic eruptions dominate the OHC changes in the deeper ocean and prevent its recovery during the

Sun and volcanoes: effect on the troposphere in the DM

J. G. Anet et al.

Title Page

Abstract

Introduction

Conclusions

References

Tables

Figures

⏪

⏩

◀

▶

Back

Close

Full Screen / Esc

Printer-friendly Version

Interactive Discussion



DM. Finally, the simulations suggest that the volcanic eruptions during the DM had a significant impact on the precipitation patterns caused by a widening of the Hadley cell and a shift of the intertropical convergence zone.

1 Introduction

5 The Dalton Minimum (DM) was a 60 yr long period of low solar activity, lasting from 1780 AD to 1840 AD. In addition, early in the 19th century, two major volcanic eruptions took place, ejecting large amounts of sulfur dioxide into the stratosphere, which, after conversion to sulfate aerosols, increased planetary albedo affecting global climate. In 1816, an exceptionally cold summer was recorded in Western Europe. This
10 year got known as the “year without summer” (Harington, 1992; Robock, 1994). While the scientific acceptance of a significant climate impact from volcanic eruptions is high, there is ongoing debate about the contribution of the solar variability to global temperature changes in the troposphere during the DM, see for example Table 2.11 of the last IPCC report (Intergovernmental Panel on Climate Change, IPCC, Climate change
15 2007, 2007).

It is well-known that solar activity varies over time. This is not only documented by the sunspot number datasets (Wolf, 1861), but also by the cosmogenic isotopes of ^{10}Be conserved in ice sheets (Steinhilber et al., 2008, 2009). The past evolution of the solar irradiance has been reconstructed by a number of authors (see Solanki et al., 2013, and references therein). Recently, Shapiro et al. (2011) reconstructed the spectral solar irradiance (SSI) for the last 400 yr using the solar modulation potential Φ as a proxy. Their results show that the decrease of the heavily absorbed UV-C during the DM reaches 15%, while it does not exceed 1% in the solar spectrum with $\lambda > 250$ nm and is negligible in the solar near infrared (NIR). This disproportionate change in the
20 spectral solar irradiance has complex effects on Earth’s atmospheric chemistry and climate system: on one hand, a substantial decrease in the UV-C at $\lambda < 250$ nm cools down the middle atmosphere and decreases the ozone production due to decelerated
25

Sun and volcanoes: effect on the troposphere in the DM

J. G. Anet et al.

Title Page

Abstract

Introduction

Conclusions

References

Tables

Figures

⏪

⏩

◀

▶

Back

Close

Full Screen / Esc

Printer-friendly Version

Interactive Discussion



Sun and volcanoes: effect on the troposphere in the DM

J. G. Anet et al.

[Title Page](#)

[Abstract](#)

[Introduction](#)

[Conclusions](#)

[References](#)

[Tables](#)

[Figures](#)

[⏪](#)

[⏩](#)

[◀](#)

[▶](#)

[Back](#)

[Close](#)

[Full Screen / Esc](#)

[Printer-friendly Version](#)

[Interactive Discussion](#)

GCRs are partly deflected by the solar wind, and therefore are negatively correlated with solar activity. Ionization of neutral molecules like N_2 or O_2 by energetic particles facilitates the formation of NO_x and HO_x (see e.g. Sinnhuber et al., 2012) accelerating the ozone destruction followed by a cooling inside the polar vortex and an increase of pole-to-equator temperature gradients, which in turn can change the tropospheric climate. These processes were simulated by several CCM and significant response of the atmosphere to EPP was identified (Calisto et al., 2011; Semeniuk et al., 2011; Rozanov et al., 2012b). However, in our previous study (Anet et al., 2013) the net effect of particles was found to be rather weak. This is seemingly contradictory, but can be partly explained by a compensating effect of decreasing LEE and increasing GCR intensity during the DM, which above-mentioned studies could not take into account because they either investigated only one sort of the energetic particles, or they compared model runs with all EPP included against a reference run without any EPP.

A third factor, which notably influenced the stratospheric and tropospheric climate and chemistry at least for a short time in the DM, are major volcanic eruptions, which are known for having ejected up to 60 Mt (Tambora volcanic eruption, year 1815) of sulfur dioxide into the atmosphere. Presumably, the plumes reached deep into the stratosphere, where the massive amounts of sulfur dioxide were converted to sulfate aerosols. As the result, the haze in the sky and colorful sunsets were reported during the period (see e.g. Olson et al., 2004). The aerosol particles efficiently scatter a fraction of the incoming solar radiation back to space, but also absorb a part of the outgoing terrestrial infrared (IR) and incoming solar near IR (NIR). The reduction in incoming visible or NIR radiation overwhelms the IR absorption, leading to an overall global cooling, except in the polar night, where sunlight is lacking and a small warming prevails (Robock, 2000). Generally, a significant cooling of the surface occurs in the first weeks after major volcanic eruptions, lasting for one to two years and leading to modified patterns of precipitation, surface pressure and the teleconnection patterns, such as the Arctic Oscillation (AO), North Atlantic Oscillation (NAO) (Shindell et al.,

2000; Stenchikov et al., 2002; Fischer et al., 2007) or the El Niño Southern Oscillation (ENSO) (Robock and Mao, 1995; Adams et al., 2003).

Different modeling studies in the recent past show a large range of simulated climate responses to solar forcings. For instance, Wagner and Zorita (2005) showed with an atmosphere–ocean general circulation model (AO-GCM) without coupled chemistry that the combined effects of volcanic eruptions and solar irradiance decrease could significantly (by up to several tenths of a degree) modify global mean temperatures. They attributed most of this cooling to the volcanic effects, and their “solar-only” simulation without volcanic eruptions showed a decrease of global temperatures of only 0.1 K. Feulner (2011) concluded from their experiment with an intermediate complexity model that the solar contribution to the cool period during the DM was likely a smaller one. They showed that the cold climate was explained mostly by volcanic forcing. Their application of the strong solar irradiance forcing proposed by Shapiro et al. (2011) led to a substantial disagreement of their simulated and the reconstructed temperature time series. Shindell et al. (2000) compared the long-term influence of volcanic eruptions to grand solar minimum conditions with focus on the DM and on the Maunder Minimum (MM) – which occurred about 150 yr before the DM. They concluded that volcanic eruptions have rather strong but only short-lived effects on temperatures, while the reduction of the solar irradiance during the grand minimum affects temperatures on longer time scales. They estimated a solar induced cooling during the MM of globally 0.6 to 0.8 K. For the same period, Varma et al. (2012) investigated the southern hemispheric wind field response to the MM solar irradiance decrease. They estimated the stratospheric ozone change due to the reduction of solar UV irradiance from a global scaling with total solar irradiance (TSI) variations, which could lead to a shift in the southern hemispheric westerly winds to the north via the “top-down” mechanism consisting of a chain of complex radiative-dynamical processes (Meehl et al., 2008; Haigh, 1996). In another paper, Varma et al. (2011) concluded that the “bottom-up” mechanism via a reduction of visible irradiance had a similar effect. However, these publications (Varma et al., 2011, 2012) do not provide detailed information on changes in tropospheric temperatures.

Sun and volcanoes: effect on the troposphere in the DM

J. G. Anet et al.

Title Page

Abstract

Introduction

Conclusions

References

Tables

Figures



Back

Close

Full Screen / Esc

Printer-friendly Version

Interactive Discussion



Sun and volcanoes: effect on the troposphere in the DM

J. G. Anet et al.

[Title Page](#)

[Abstract](#)

[Introduction](#)

[Conclusions](#)

[References](#)

[Tables](#)

[Figures](#)

[⏪](#)

[⏩](#)

[◀](#)

[▶](#)

[Back](#)

[Close](#)

[Full Screen / Esc](#)

[Printer-friendly Version](#)

[Interactive Discussion](#)

The influence of volcanic and solar forcing on ozone chemistry, stratospheric temperatures and global circulation has become of great scientific interest in the recent years. The aim of this work is to analyze the tropospheric climate changes during the DM with a fully coupled atmosphere–ocean chemistry-climate model (AO-CCM) driven by the state-of-the-art set of climate forcings and to disentangle the contributions from changes in solar spectral irradiance, energetic particles and volcanic eruptions. To the best of our knowledge so far, such a sophisticated model and climate forcing set have not been applied for the evaluation of the tropospheric climate changes during the DM.

The work is structured as follows: after Sect. 1, which described the state of the research and introduced some notation, Sect. 2 will provide a description of our model and our experiments. Section 3 focuses on the changes in surface temperatures and precipitation patterns caused by the different forcings. We further compare our model results to reconstructed temperature fields, and conclude in Sect. 4.

2 Sensitivity experiments and model description

2.1 AO-CCM SOCOL3-MPIOM

The AO-CCM SOCOL3-MPIOM emerges from a modification of CCM SOCOL version 3 (Stenke et al., 2013), which has been coupled with the OASIS3 coupler (Valcke, 2013) to the Max Planck Institute ocean model (Marsland et al., 2003). SOCOL3 is based on the GCM ECHAM5 (Roeckner et al., 2003) and includes the chemical part of the chemistry-transport model MEZON (Rozanov et al., 1999; Egorova et al., 2003; Schraner et al., 2008). SOCOL3-MPIOM is applied in middle atmosphere mode (MA) extending from the ground to 0.01 hPa or around 80 km. Simultaneously with the radiation calculation, MA-ECHAM5 hands over temperature fields to MEZON, which takes into account interactions between 41 gas species – including 200 gas phase, 16 heterogeneous and 35 photolytic reactions. Those chemical fields are then handed back

Sun and volcanoes: effect on the troposphere in the DM

J. G. Anet et al.

Title Page

Abstract

Introduction

Conclusions

References

Tables

Figures

⏪

⏩

◀

▶

Back

Close

Full Screen / Esc

Printer-friendly Version

Interactive Discussion

the solar variability, on which the 11 yr activity cycle calculated from the sunspot number is then superposed. The time-dependent solar spectral irradiance is derived using a state-of-the-art radiation code COSI (Shapiro et al., 2010). The resulting spectral solar irradiance of this reconstruction is substantially lower during the MM than the one observed today, and the difference is larger than in the other recently published estimates. The advantage of this high-amplitude reconstruction is that it allows us to derive a maximum conceivable terrestrial climate response to solar changes, while other reconstructions leave hardly any fingerprint in the modeled climate.

For the EPPs, the A_p index reconstruction from Baumgaertner et al. (2009) is used for the LEE. For SEPs, return-period based datasets were created from an analysis of the last 45 yr of the last century. The GCR ionization rates depend on Φ (Fig. 1c), which was reconstructed by Steinhilber et al. (2008). The geomagnetic dipole field strength and position is provided from paleomagnetic datasets from Finlay et al. (2010).

The volcanic forcing is based on simulations carried with a 2-D aerosol microphysical model (Arfeuille et al., 2013). It uses total aerosol injection values from Gao et al. (2008) and information on date/location of each eruptions. The stratospheric aerosols are prescribed in terms of extinction ratios, single scattering albedos and asymmetry factors for each of the 22 ECHAM5 radiation bands and in terms of surface area densities, for each latitude-altitude band of SOCOL (zonally averaged). Aerosol optical depth values derived from this forcing are documented in Table 1. The globally averaged effect on incoming surface shortwave radiation is shown in Fig. 1d.

The QBO was generated by means of a backwards extension of an already existing reconstruction, using an idealized QBO cycle which is superimposed onto the regular seasonal cycle (Brönnimann et al., 2007).

The greenhouse gas forcing (Fig. 1e) forcing for the period from 1780 to 1840 are based on the PMIP3 protocol (Etheridge et al., 1996, 1998; Ferretti et al., 2005; MacFarling-Meure et al., 2006; Meehl et al., 2009) while halogens are kept constant at preindustrial levels. The standard ECHAM5 land surface datasets by Hagemann et al. (1999) and Hagemann (2002) are used. Tropospheric aerosol fields were extracted

from existing CAM3.5 simulations driven by CCSM3 (CMIP4) sea-surface temperatures and 1850–2000 CMIP5 emissions. These fields were then scaled as a function of the world population starting in the year 1850 going backwards, except for the 10 % (relative to the 1990 values) of biomass burning, which were considered constant over time.

For the global CO and NO_x emissions, the part emitted from shipping was calculated starting from the CMIP5 datasets, which were projected linearly backwards from 1850 on to the year 1800. Before 1800, no steamships existed, thus these emissions were set to zero. The natural biomass burning emissions were assumed to be constant over time, while the anthropogenic biomass burning emissions were scaled with the world population. The emissions are illustrated in Fig. 1f.

2.3 Sensitivity experiments

We performed six sensitivity experiments covering the time period from 1780 to 1840 (Table 2), each with three ensemble members. These simulations are identical to those described by Anet et al. (2013). The nomenclature is as follows: the run including all effects acting together on the climate system is named ALL. The sensitivity experiment “Top-Down” (TD, Meehl et al., 2008) experiment includes only the variations of solar irradiance with $\lambda < 250$ nm and the corresponding extra heating (corrections for the Lyman- α line, the Schumann–Runge, Hartley and Huggins bands) and photolysis rates of photolytic chemical reactions. The “Bottom-Up” (BU) experiment (Meehl et al., 2008) allows only irradiance $\lambda > 250$ nm to vary over time. The EPP experiment is exclusively forced by energetic particles. In the VOLC experiment, all other forcings except the stratospheric aerosols, which affect the radiation budget and heterogeneous chemistry via changes in surface area density (SAD), were kept constant. All runs were compared to a control run with perpetual 1780 conditions called CTRL1780. The analysis of the data was done by comparing zonally and temporally averaged ensemble mean fields to the CTRL1780 ensemble mean.

Sun and volcanoes: effect on the troposphere in the DM

J. G. Anet et al.

Title Page

Abstract

Introduction

Conclusions

References

Tables

Figures



Back

Close

Full Screen / Esc

Printer-friendly Version

Interactive Discussion

cooling during northern hemispheric (NH) winter over Siberia and Alaska, as well as the significant warming during polar winter over the respective polar hemisphere (Fig. S1).

The cooling of the continents can be explained by the BU experiment shown in Fig. 2b, which simulates cooling patterns similar to the ALL ensemble mean, except over northern Asia and parts of Europe. The cooling is caused by the negative anomaly in solar irradiance at wavelengths $\lambda > 250$ nm and subsequently by a reduced heating of the surface. The weaker ocean response is related to the large heat capacity of the ocean, partly compensating the reduced irradiance. The Siberian cold anomaly could be related to an increasing snow cover during the cold season, leading to a negative albedo feedback.

The slight warming anomalies over the Bering Sea and western Antarctic Peninsula regions can be explained with the VOLC simulation (Fig. 2c). The warming pattern over the Bering Sea region, triggered by ocean upwelling (see later) is present during the whole year. In the western Antarctic Peninsula and North Atlantic regions, the patterns are predominant during the SH winter season (JJA). The western Antarctic Peninsula warming is associated with an enhanced transport of milder air masses from the subtropics. This is related to differential temperature anomalies from absorption and/or reflection of radiation by the volcanic aerosols, as shown in Anet et al. (2013). The major warming over the Bering Sea originates from a strengthening of the northward surface winds inducing a positive meridional wind stress anomaly above the northwestern Pacific and the opposite – namely a weakening of the northward surface winds inducing a negative anomaly of the meridional wind stress – in the northeastern Pacific region (not shown). This facilitates ocean upwelling via the Ekman mechanism at this region, where deep water upwelling prevails (oceanic conveyor belt). The surface water of the northern Bering Sea region, cooling down during the winter season, is being replaced by deeper, older water from the thermocline region, which has no imprint of the volcanic signal yet, as indicated by a slight increase of the modeled vertical ocean mass transport in the winter season in that region. The warming signal is being so strong that it persists throughout the year. This result, though it seems consistent, should be

CPD

9, 6179–6220, 2013

Sun and volcanoes: effect on the troposphere in the DM

J. G. Anet et al.

Title Page

Abstract

Introduction

Conclusions

References

Tables

Figures

⏪

⏩

◀

▶

Back

Close

Full Screen / Esc

Printer-friendly Version

Interactive Discussion

region. The exact reason of this different behavior has not yet been found, but origins likely in a weaker winter vortex in SOCOL3-MPIOM. The deficiency is confirmed by the lack of any significant temperature response to the TD and EPP signal over Europe – which could possibly be improved by modifying the gravity wave parameterization in ECHAM5.

In agreement with Robock and Mao (1992), Kirchner et al. (1999), and Driscoll et al. (2012), or to the DM analysis of Fischer et al. (2007), we discern a significant winter warming pattern (WWP) over Europe, Russia and parts of Northern America in the years following the volcanic eruptions (Fig. 3b) and a cool anomaly during the summer seasons following the volcanic eruptions (Fig. 3a). The warming in DJF is caused by a slight shift of the NAO to a NAO+-like phase, enhancing the westerlies (see Fig. 3d) and influences the precipitation patterns (see later). The axis of the NAO pattern is slightly tilted counterclockwise (see climatology in Fig. S3).

We now focus on the temporal evolution of the temperature anomalies during the DM (Fig. 4). For these illustrations, values of the CTRL1780 experiment were subtracted from the ALL, VOLC and BU time series. The internal variability of CTRL1780 is relatively small (σ global, annual ensemble mean (AEM) = 0.095, σ NH AEM = 0.154, σ SH AEM = 0.099).

Compared to CTRL1780 the ALL experiment (Fig. 4a) shows a significant decrease in global mean temperatures starting in 1809. After the temperature minimum following the Tambora eruption (1815) the modeled temperatures show a slight recovery, but do not completely reach normal condition. After 1830, a second decrease in temperatures follows. We note that before 1809, all experiments show a very similar temperature evolution and that the strong volcanic eruptions (1809, 1815, 1831 and 1835), cause a clear excursion to low temperatures. These signals are clearly visible in the ocean heat content (Fig. 4b). Again, four short-term reductions in the ALL run can be recognized after the volcanic eruptions, however with a delay of 2 to 4 yr due to the thermal inertia of the ocean. Until 1830 the SH mean temperature evolution (Fig. 4c) is very similar to the global mean. However, the volcanic eruptions after 1830 have a smaller

Sun and volcanoes: effect on the troposphere in the DM

J. G. Anet et al.

Title Page

Abstract

Introduction

Conclusions

References

Tables

Figures



Back

Close

Full Screen / Esc

Printer-friendly Version

Interactive Discussion

Sun and volcanoes: effect on the troposphere in the DM

J. G. Anet et al.

[Title Page](#)

[Abstract](#)

[Introduction](#)

[Conclusions](#)

[References](#)

[Tables](#)

[Figures](#)

[⏪](#)

[⏩](#)

[◀](#)

[▶](#)

[Back](#)

[Close](#)

[Full Screen / Esc](#)

[Printer-friendly Version](#)

[Interactive Discussion](#)

influence on SH temperatures, as the Babuyan Claro (1831) and Cosiguina (1835) eruptions are of smaller size than the 1809 and 1815 eruptions and also characterized by a higher aerosol loading in the NH than in the SH. Due to the smaller direct aerosol forcing and to the much higher internal variability of the climate system in the NH than in the SH, the cooling signal after 1809 is far more difficult to recognize in Fig. 4d. However, a significant decrease in temperatures of the ALL experiment is simulated after 1815 as well a second dip to lower temperatures drop after 1830.

The cooling after 1809 can be partially explained by the volcanic eruptions of 1809, 1815, 1831 and 1835. The green curve in Fig. 4a and b of the VOLC experiment shows negative excursions at exactly those years. However, a clear recovery to pre-1809 temperatures is simulated after 1817. The next decrease in temperatures appears only after the 1831 volcanic eruption. Focusing on the volcanic response a clear inter-hemispheric difference is found: while in the SH, especially the 1809 and 1815 volcanic eruptions are well visible, the NH seems to be more responsive to the 1831 and 1835 volcanic eruptions. This is consistent with the different stratospheric aerosol loading. The temperature increase in the NH from 1813 to 1820 back to unperturbed temperature levels – and even positive anomalies in the 1820s – represents a supercompensation-like feature simulated by our model after each strong volcanic eruption. As it will be shown later, this warm anomaly pattern is caused by oceanic influence. The short-term warming right after preindustrial volcanic eruptions can be explained by a small, but significant increase in tropospheric ozone concentrations after the volcanic eruptions, acting as a greenhouse gas. This increase of ozone is related to a reduction of the production rate (less radiation, less water vapour) of the hydroxyl radical OH, which is a very efficient factor of the ozone destruction. This increase is especially pronounced over the NH due to larger CO concentrations.

In order to explain the rather low temperatures of ALL between 1817 and 1830, an additional mechanism to the volcanic eruptions only has to be considered: the BU ensemble mean in Fig. 4a and b describes a negative anomaly in temperatures and OHC from 1808 on. Those below-normal conditions persist until the year 1839, and are

by far stronger in the NH (Fig. 4d) than in the SH (Fig. 4c) due to greater amount of land masses. Our model results even suggest an unprecedented cool period in the NH in the 1820s following the BU scenario. This period would even have been colder than the simulated and reconstructed (see later) post-Tambora era (1816–1818), hence pointing at the importance of the volcanic eruptions during the DM, which interfered with the solar-only forcing effects.

In the ocean, a downward propagation of the signal from shallow to more deep layers is illustrated in Fig. 5a–c. While neither radiation with $\lambda < 250$ nm nor EPP (Fig. S4) seem to significantly influence the ocean heat content at any level, the radiation with $\lambda > 250$ nm (Fig. 5b) and volcanic (Fig. 5c) signals propagate down to deeper ocean layers. In Fig. 5a, we note that while the upper layers (green curves) still show a small recovery after the volcanic eruptions, taking around 5–8 yr, there is no signal of recovery in the deep ocean (black curves) during the DM period. Moreover, on one hand, the bottom-up signal (Fig. 5b) takes more time to influence the ocean heat content in deeper layers than the volcanic eruptions (Fig. 5c), which is due to the lower net irradiance anomaly in the solar forcing than in the volcanic forcing. On the other hand, the persistence of the BU-signal among all layers is more constant than the volcanic imprint due to the lack of “peaks” of activity. Still, the BU-scenario is only the second strongest contributor to changes in the deep-layer ocean heat content, ranging behind the volcanic eruptions. One should especially note that while the uppermost layers of the VOLC experiment recover quite quickly (Fig. 5c, green curve), the signal stays memorized in the ocean, being rapidly transported into deeper layers (Fig. 5c, black curve).

Globally, a superrecovery of OHC during the 1820s is simulated for the VOLC experiment: this positive anomaly can be explained when focusing on the Bering Sea region (Fig. 5d), which can explain more than half of the global ocean heat content increase by the volcanic contribution.

Stenchikov et al. (2009) also investigated the influence of the Tambora eruption on the ocean. For all layers our simulated OHC anomaly is more pronounced, which can be explained by the lack of the 1809 volcanic eruption in the work of Stenchikov et al.

Sun and volcanoes: effect on the troposphere in the DM

J. G. Anet et al.

[Title Page](#)

[Abstract](#)

[Introduction](#)

[Conclusions](#)

[References](#)

[Tables](#)

[Figures](#)

[⏪](#)

[⏩](#)

[◀](#)

[▶](#)

[Back](#)

[Close](#)

[Full Screen / Esc](#)

[Printer-friendly Version](#)

[Interactive Discussion](#)

lished in the Intergovernmental Panel on Climate Change, IPCC, Climate change 2007 (2007), in order to allow comparison with other, similar modeling studies (e.g. Wagner and Zorita, 2005). We focus on NH temperature reconstructions since the density of proxy data is higher over the NH than over the SH and, therefore, NH data are expected to be more reliable. In Fig. S4, the five different reconstructions of the NH temperatures used in this work are illustrated (Jones et al., 2001; Esper et al., 2002; D'Arrigo et al., 2006; Briffa et al., 2001; Mann et al., 1999).

In Fig. 6, the temperature evolution of the NH 2 m temperatures of the ALL, VOLC and BU experiments is compared to reconstructions, represented by a grey envelope. The general anomaly pattern shown for the ALL experiment, that means, positive anomalies until the beginning of the 19th century, followed by a strong cooling between 1810 and 1820, a warmer period in the 1820s and a further temperature minimum around 1835, agrees very well with the reconstructed temperatures.

The first 30 yr of the ALL time series are characterized by a slight temperature decrease, overlain by the 11 yr solar cycle. As obvious from the sensitivity run BU, the temperatures follow the decline in solar irradiance of the Shapiro et al. (2011) forcing (Fig. 6, top panel). The cooling after the two smaller volcanic eruptions in the 1790s overcompensates the pure solar signal. While most of the reconstructions also show a 11 yr-like cycle (Fig. S5), the dating of the minima and maxima differs among the data sets, leading to a rather diffuse picture.

Starting from around 1805 until 1816 both the reconstructions and the modeled temperatures show a strong cooling by up to 0.6 K. During that period, the ALL experiment is in very good agreement with the composite of the reconstructions, although a slight overestimation of the 1809 volcanic induced cooling in 1811–1812 is visible. After the two major volcanic eruptions in 1809 and 1815, the temperatures in the ALL experiment show a clear recovery until the year 1826. A very similar behavior is observed in the reconstructions, although the warming in the 1820s is stronger than in the ALL simulation. As can be seen from the sensitivity runs BU and VOLC, the simulated temperature behavior can be explained as a combination of solar and volcanic effects: the

CPD

9, 6179–6220, 2013

Sun and volcanoes: effect on the troposphere in the DM

J. G. Anet et al.

Title Page

Abstract

Introduction

Conclusions

References

Tables

Figures

⏪

⏩

◀

▶

Back

Close

Full Screen / Esc

Printer-friendly Version

Interactive Discussion

Sun and volcanoes: effect on the troposphere in the DM

J. G. Anet et al.

Title Page

Abstract

Introduction

Conclusions

References

Tables

Figures

⏪

⏩

◀

▶

Back

Close

Full Screen / Esc

Printer-friendly Version

Interactive Discussion

BU experiment shows that the solar-only driven cooling starts already around 1803, but the overall cooling is slightly postponed by a compensating warming by the earlier volcanic eruptions. The eruption of Mt. Tambora in 1815 overcompensates the solar induced warming after 1810, leading to a temperature minimum around 1816/1817, while the solar minimum around 1822 (BU) prevents a more pronounced warming during the 1820s as visible in the model experiment VOLC.

The two volcanic eruptions of 1831 and 1835 with a predominant NH aerosol loading are followed by a second pronounced cold period, which is visible in the model simulations as well as in the reconstructions. Also, the simulated amplitude of this cooling with 0.3–0.4 K is similar to the reconstructions.

Finally, the model simulation shows a warming after 1836, which can be explained by a general increase in solar irradiance at the end of the DM as well as dilution and removal of volcanic aerosols in the stratosphere. The warming is also found in the reconstructions.

It should be mentioned that the separation of solar and volcanic effects as done in BU and VOLC neglects non-linear feedbacks. Nevertheless, we conclude that only the combination of both volcanic events and BU decrease is able to reproduce the reconstructed temperature patterns. Moreover, we suggest that a solar-only driven DM would have induced two cold periods in the 1810s and 1820s. Those were overcompensated by a strong VOLC warming signal in the ALL temperature pattern.

3.3 Precipitation and tropospheric circulation

Figure 7 illustrates the absolute difference in seasonal averaged precipitation (JJA and DJF) for the ALL and VOLC run relative to the constant forcing run CTRL1780. As can be recognized, the intertropical convergence zone (ITCZ) is shifted northwards to the equatorial Atlantic. Furthermore, a sharp decrease in precipitation both during the boreal summer and winter is modeled over the “El Niño” region, eastern Central America, and the maritime continent.

Sun and volcanoes: effect on the troposphere in the DM

J. G. Anet et al.

[Title Page](#)

[Abstract](#)

[Introduction](#)

[Conclusions](#)

[References](#)

[Tables](#)

[Figures](#)

[⏪](#)

[⏩](#)

[◀](#)

[▶](#)

[Back](#)

[Close](#)

[Full Screen / Esc](#)

[Printer-friendly Version](#)

[Interactive Discussion](#)

that the signal disappears in the rather high noise of the NH temperature signal. The underestimation of the solar UV irradiance changes suggested by Shapiro et al. (2011) in comparison with the latest satellite measurements (Ermolli et al., 2013) could also be a reason, because a stronger UV forcing can make the top-down mechanism more efficient (see e.g. Ineson et al., 2011). The other unexpected result is the weak influence of energetic particles which can be explained by the absence of ozone response to the effects of low energy electrons discussed by Anet et al. (2013) and probably some compensation between enhanced ionization by GCR and depressed ionization by electrons and protons during the DM.

We also show that due to volcanic eruptions, the hydrological cycle can be perturbed as such to decelerate the Hadley and Ferrel cells for a certain time. At the same time, the NAO is pushed into a NAO+-like phase in the winters following a volcanic eruption, leading to an increase in precipitation in northern Europe and a negative precipitation anomaly in southern Europe. Still, the precipitation anomaly is weaker than in other publications cited in our manuscript.

It is possible that our chosen timing in the volcanic forcing data (date of the year) of the 1809 and 1831 eruptions are wrong. This could of course influence the results discussed in the manuscript, as the timing (in the year) of the eruption determines in which hemisphere most of the volcanic aerosol will be transported. Moreover, characteristics of the stratospheric dynamics in the DM – such as the QBO which was nudged in our model and in the volcanic forcing calculation – are only reconstructed, and not observed. Also here, a certain margin of uncertainty persists, possibly influencing our results. The anomalies in temperature and precipitation might be more significant, as only two month of difference in the volcanic eruption lead to different results (as stated and shown in e.g. Kravitz and Robock, 2011; Toohey et al., 2011; Driscoll et al., 2012).

This is also a reason why the upwelling mechanism in the Bering Sea region, leading to the overcompensation-like temperature signal after the strong volcanic eruptions should be considered with interest, but with care. A different timing of the eruptions might lead to a different reaction not only of the tropospheric circulation cells, but also

of the ocean. Also, internal variability might be a reason for the simulated response of the Bering Sea region.

Future investigations should be done focusing on the downward propagation of the stratospheric perturbations in a model with prescribed sea surface temperatures vs. a model with interactive ocean. As well future research should investigate to what extent the impact of decreasing SEP/LEE efficiency can compensate increasing GCR influences on regional temperature changes. The upwelling signal in the Bering Sea region should be confirmed with a different timing of the volcanic eruptions and another model setup. Moreover, the statistical testing procedures should be consolidated by increasing the number of ensemble members.

Supplementary material related to this article is available online at <http://www.clim-past-discuss.net/9/6179/2013/cpd-9-6179-2013-supplement.zip>.

Acknowledgements. Support by Swiss National Science Foundation under the grant CRSI122-130642 (FUPSOL) is gratefully acknowledged. Moreover, we would like to acknowledge the NCL plotting tool (NCAR/CISL/VETS, 2012), which enabled efficient and appealing visualization of the model data. E. Rozanov, A. I. Shapiro, and W. Schmutz thank COST Action ES1005 TOSCA (<http://www.tosca-cost.eu>) for the support and fruitful discussions. Many thanks go also to H. Wanner (Oeschger Centre for Climate Change Research, Bern) for the efficient, creative and enthusiastic discussions.

**Sun and volcanoes:
effect on the
troposphere in the
DM**

J. G. Anet et al.

Title Page

Abstract

Introduction

Conclusions

References

Tables

Figures



Back

Close

Full Screen / Esc

Printer-friendly Version

Interactive Discussion



Sun and volcanoes: effect on the troposphere in the DM

J. G. Anet et al.

Title Page

Abstract

Introduction

Conclusions

References

Tables

Figures

⏪

⏩

◀

▶

Back

Close

Full Screen / Esc

Printer-friendly Version

Interactive Discussion

- Cecile, J., Pagnutti, C., and Anand, M.: A likelihood perspective on tree-ring standardization: eliminating modern sample bias, *Clim. Past Discuss.*, 9, 4499–4551, doi:10.5194/cpd-9-4499-2013, 2013. 6196
- D'Arrigo, R., Wilson, R., and Jacoby, G.: On the long-term context for late twentieth century warming, *J. Geophys. Res.*, 111, D03103, doi:10.1029/2005JD006352, 2006. 6197
- Driscoll, S., Bozzo, A., Gray, L. J., Robock, A., and Stenchikov, G.: Coupled Model Intercomparison Project 5 (CMIP5) simulations of climate following volcanic eruptions, *J. Geophys. Res.-Atmos.*, 117, D17105, doi:10.1029/2012JD017607, 2012. 6193, 6202
- Egorova, T., Rozanov, E., Zubov, V., and Karol, I.: Model for Investigating Ozone Trends (MEZON), *Izvestiia Akademii Nauk SSSR, Ser. Fiz. Atmos. Okean.*, 39, 310–326, 2003. 6186
- Egorova, T., Rozanov, E., Manzini, E., Haberreiter, M., Schmutz, W., Zubov, V., and Peter, T.: Chemical and dynamical response to the 11 yr variability of the solar irradiance simulated with a chemistry-climate model, *Geophys. Res. Lett.*, 31, L06119, doi:10.1029/2003GL019294, 2004. 6187
- Ermolli, I., Matthes, K., Dudok de Wit, T., Krivova, N. A., Tourpali, K., Weber, M., Unruh, Y. C., Gray, L., Langematz, U., Pilewskie, P., Rozanov, E., Schmutz, W., Shapiro, A., Solanki, S. K., and Woods, T. N.: Recent variability of the solar spectral irradiance and its impact on climate modelling, *Atmos. Chem. Phys.*, 13, 3945–3977, doi:10.5194/acp-13-3945-2013, 2013. 6202
- Esper, J., Cook, E. R., and Schweingruber, F. H.: Low-frequency signals in long tree-ring chronologies for reconstructing past temperature variability, *Science*, 295, 2250–2253, doi:10.1126/science.1066208, 2002. 6197
- Etheridge, D., Steele, L., Langenfelds, R., Francey, R., Barnola, J., and Morgan, V.: Natural and anthropogenic changes in atmospheric CO₂ over the last 1000 yr from air in Antarctic ice and firn, *J. Geophys. Res.*, 101, 4115–4128, doi:10.1029/95JD03410, 1996. 6188
- Etheridge, D. M., Steele, L. P., Francey, R. J., and Langenfelds, R. L.: Atmospheric methane between 1000 AD, and present: evidence of anthropogenic emissions and climatic variability, *J. Geophys. Res.*, 103, 15979–15993, doi:10.1029/98JD00923, 1998. 6188
- Ferretti, D., Miller, J., White, J., Etheridge, D., Lassey, K., Lowe, D., Meure, C., Dreier, M., Trudinger, C., Van Ommen, T., and Langenfelds, R.: Unexpected changes to the global methane budget over the past 2000 yr, *Science*, 309, 1714–1717, doi:10.1126/science.1115193, 2005. 6188

Sun and volcanoes: effect on the troposphere in the DM

J. G. Anet et al.

[Title Page](#)

[Abstract](#)

[Introduction](#)

[Conclusions](#)

[References](#)

[Tables](#)

[Figures](#)

[⏪](#)

[⏩](#)

[◀](#)

[▶](#)

[Back](#)

[Close](#)

[Full Screen / Esc](#)

[Printer-friendly Version](#)

[Interactive Discussion](#)

Ineson, S., Scaife, A. A., Knight, J. R., Manners, J. C., Dunstone, N. J., Gray, L. J., and Haigh, J. D.: Solar forcing of winter climate variability in the Northern Hemisphere, *Nature*, 4, 753–757, doi:10.1038/NCEO1282, 2011. 6202

Intergovernmental Panel on Climate Change, IPCC: Climate Change 2007: the Physical Science Basis, Contribution of Working Group I to the Fourth Assessment Report of the Intergovernmental Panel on Climate Change, in: AR4, edited by: Solomon, S., Qin, D., Manning, M., Chen, Z., Marquis, M., Averyt, K., Tignor, H., and Miller, H., Cambridge University Press, Cambridge, UK, and New York, NY, USA, 2007. 6182, 6197

Jones, P. D., Ogilvie, A. E., Davies, T. D., and Briffa, K. R.: History and Climate: Memories of the Future?, Springer, New York, 2001. 6196, 6197

Kirchner, I., Stenchikov, G. L., Graf, H.-F., Robock, A., and Antuna, J. C.: Climate model simulation of winter warming and summer cooling following the 1991 Mount Pinatubo volcanic eruption, *J. Geophys. Res.*, 104, 19039–19055, doi:10.1029/1999JD900213, 1999. 6193, 6200

Kodera, K. and Kuroda, Y.: Dynamical response to the solar cycle, *J. Geophys. Res.*, 107, 4749–4761, doi:10.1029/2002JD002224, 2002. 6183

Kravitz, B. and Robock, A.: Climate effects of high-latitude volcanic eruptions: role of the time of year, *J. Geophys. Res.*, 116, D01105, doi:10.1029/2010JD014448, 2011. 6202

Labitzke, K., Austin, J., Butchart, N., Knight, J., Takahashi, M., Nakamoto, M., Nagashima, T., Haigh, J., and Williams, V.: The global signal of the 11 yr solar cycle in the stratosphere: observations and models, *J. Atmos. Sol.-Terr. Phys.*, 64, 203–210, doi:10.1016/S1364-6826(01)00084-0, 2002. 6183

Luterbacher, J., Dietrich, D., Xoplaki, E., Grosjean, M., and Wanner, H.: European seasonal and annual temperature variability, trends, and extremes since 1500, *Science*, 303, 1499–1503, doi:10.1126/science.1093877, 2004. 6200

MacFarling-Meure, C., Etheridge, D., Trudinger, C., Steele, P., Langenfelds, R., Van Ommen, T., Smith, A., and Elkins, J.: Law dome CO₂, CH₄ and N₂O ice core records extended to 2000 yr BP, *Geophys. Res. Lett.*, 33, L14810, doi:10.1029/2006GL026152, 2006. 6188

Mann, M., Bradley, S., and Hughes, M.: Northern Hemisphere temperatures during the past millennium: inferences, uncertainties, and limitations, *Geophys. Res. Lett.*, 26, 759–762, doi:10.1029/1999GL900070, 1999. 6197

Sun and volcanoes: effect on the troposphere in the DM

J. G. Anet et al.

Title Page

Abstract

Introduction

Conclusions

References

Tables

Figures

⏪

⏩

◀

▶

Back

Close

Full Screen / Esc

Printer-friendly Version

Interactive Discussion

- Mann, M. E., Fuentes, J. D., and Rutherford, S.: Underestimation of volcanic cooling in tree-ring-based reconstructions of hemispheric temperatures, *Nat. Geosci.*, 5, 202–205, doi:10.1038/ngeo1394, 2012. 6196
- Marsland, S., Haak, H., Jungclaus, J., Latif, M., and Roske, F.: The Max-Planck-Institute global ocean/sea ice model with orthogonal curvilinear coordinate, *Ocean Model.*, 5, 91–27, doi:10.1016/S1463-5003(02)00015-X, 2003. 6186
- McGregor, S. and Timmermann, A.: The effect of explosive tropical volcanism on ENSO, *J. Climate*, 24, 2178–2191, doi:10.1175/2010JCLI3990.1, 2011. 6199
- Meehl, G., Arblaster, J., Branstator, G., and Van Loon, H.: A coupled air–sea response mechanism to solar forcing in the Pacific region, *J. Climate*, 21, 2883–2897, doi:10.1175/2007JCLI1776.1, 2008. 6183, 6185, 6189
- Meehl, G. A., Arblaster, J. M., Matthes, K., Sassi, F., and van Loon, H.: Amplifying the Pacific climate system response to a small 11 yr solar cycle forcing, *Science*, 325, 1114–1118, doi:10.1126/science.1172872, 2009. 6183, 6188
- NCAR/CISL/VETS: The NCAR Command Language (Version 6.0.0) [Software], Boulder, USA, 2012. 6203
- Olson, D. W., Doescher, R. L., and Olson, M. S.: The blood-red sky of the scream, 13, *American Physical Society*, Maryland, 2004. 6184
- Robock, A.: Review of year without a summer? World climate in 1816, *Climatic Change*, 26, 105–108, 1994. 6182
- Robock, A.: Volcanic eruptions and climate, *Rev. Geophys.*, 38, 191–219, doi:10.1029/1998RG000054, 2000. 6184
- Robock, A. and Mao, J.: Winter warming from large volcanic eruptions, *Geophys. Res. Lett.*, 19, 2405–2408, doi:10.1029/92GL02627, 1992. 6193, 6200
- Robock, A. and Mao, J.: The volcanic signal in surface temperature observations, *J. Climate*, 8, 1086–1103, doi:10.1175/1520-0442(1995)008<1086:TVSIST>2.0.CO;2, 1995. 6185
- Roeckner, E., Baeuml, G., Bonaventura, L., Brokopf, R., Esch, M., Giorgetta, M., Hagemann, S., Kirchner, I., Kornblueh, L., Manzini, E., Rhodin, A., Schlese, U., Schulzweida, U., and Tompkins, A.: The atmospheric general circulation model ECHAM 5, Part 1: Model description, Report No. 349, available at: http://www.mpimet.mpg.de/fileadmin/publikationen/Reports/max_scirep_349.pdf, Max-Planck-Institut für Meteorologie, Hamburg, 2003. 6186
- Rozanov, E., Schlesinger, M. E., Zubov, V., Yang, F., and Andronova, N. G.: The UIUC three-dimensional stratospheric chemical transport model: description and eval-

Sun and volcanoes: effect on the troposphere in the DM

J. G. Anet et al.

[Title Page](#)

[Abstract](#)

[Introduction](#)

[Conclusions](#)

[References](#)

[Tables](#)

[Figures](#)

[⏪](#)

[⏩](#)

[◀](#)

[▶](#)

[Back](#)

[Close](#)

[Full Screen / Esc](#)

[Printer-friendly Version](#)

[Interactive Discussion](#)

- uation of the simulated source gases and ozone, *J. Geophys. Res.*, 104, 755–781, doi:10.1029/1999JD900138, 1999. 6186
- Rozanov, E. V., Egorova, T. A., Shapiro, A. I., and Schmutz, W. K.: Modeling of the atmospheric response to a strong decrease of the solar activity, *Proc. Int. Astron. Union*, 7, 215–224, doi:10.1017/S1743921312004863, 2012a. 6183
- Rozanov, E., Calisto, M., Egorova, T., Peter, T., and Schmutz, W.: Influence of the precipitating energetic particles on atmospheric chemistry and climate, *Surv. Geophys.*, 33, 483–501, doi:10.1007/s10712-012-9192-0, 2012b. 6184, 6187, 6192
- Schraner, M., Rozanov, E., Schnadt Poberaj, C., Kenzelmann, P., Fischer, A. M., Zubov, V., Luo, B. P., Hoyle, C. R., Egorova, T., Fueglistaler, S., Brönnimann, S., Schmutz, W., and Peter, T.: Technical Note: Chemistry-climate model SOCOL: version 2.0 with improved transport and chemistry/microphysics schemes, *Atmos. Chem. Phys.*, 8, 5957–5974, doi:10.5194/acp-8-5957-2008, 2008. 6186
- Semeniuk, K., Fomichev, V. I., McConnell, J. C., Fu, C., Melo, S. M. L., and Usoskin, I. G.: Middle atmosphere response to the solar cycle in irradiance and ionizing particle precipitation, *Atmos. Chem. Phys.*, 11, 5045–5077, doi:10.5194/acp-11-5045-2011, 2011. 6184
- Shapiro, A. I., Schmutz, W., Schoell, M., Haberreiter, M., and Rozanov, E.: NLTE solar irradiance modeling with the COSI code, *Astron. Astrophys.*, 517, A48+, doi:10.1051/0004-6361/200913987, 2010. 6188
- Shapiro, A. I., Schmutz, W., Rozanov, E., Schoell, M., Haberreiter, M., Shapiro, A. V., and Nyeki, S.: A new approach to the long-term reconstruction of the solar irradiance leads to large historical solar forcing, *Astron. Astrophys.*, 529, A67, doi:10.1051/0004-6361/201016173, 2011. 6182, 6185, 6187, 6197, 6201, 6202, 6218
- Shindell, D., Schmidt, G., Miller, R., and Mann, M.: Volcanic and solar forcing of climate change during the preindustrial era, *J. Climate*, 16, 4094–4107, doi:10.1175/1520-0442(2003)016<4094:VASFOC>2.0.CO;2, 2000. 6184, 6185
- Sinnhuber, M., Nieder, H., and Wieters, N.: Energetic particle precipitation and the chemistry of the mesosphere/lower thermosphere, *Surv. Geophys.*, 33, 1281–1334, doi:10.1007/s10712-012-9201-3, 2012. 6184
- Solanki, S. K., Krivova, N. A., and Haigh, J. D.: Solar irradiance variability and climate, *Astron. Astrophys.*, 51, 311–351, doi:10.1146/annurev-astro-082812-141007, 2013. 6182
- Steinhilber, F., Abreu, J. A., and Beer, J.: Solar modulation during the Holocene, *Astrophys. Space Sci.*, 4, 1–6, doi:10.5194/astra-4-1-2008, 2008. 6182, 6188, 6213

Sun and volcanoes: effect on the troposphere in the DM

J. G. Anet et al.

[Title Page](#)

[Abstract](#)

[Introduction](#)

[Conclusions](#)

[References](#)

[Tables](#)

[Figures](#)

[⏪](#)

[⏩](#)

[◀](#)

[▶](#)

[Back](#)

[Close](#)

[Full Screen / Esc](#)

[Printer-friendly Version](#)

[Interactive Discussion](#)

- Steinhilber, F., Beer, J., and Fröhlich, C.: Total solar irradiance during the Holocene, *Geophys. Res. Lett.*, 36, L19704, doi:10.1029/2009GL040142, 2009. 6182
- Stenchikov, G., Robock, A., Ramaswamy, V., Schwarzkopf, M. D., Hamilton, K., and Ramachandran, S.: Arctic Oscillation response to the 1991 Mount Pinatubo eruption: effects of volcanic aerosols and ozone depletion, *J. Geophys. Res.*, 107, 1–16, doi:10.1029/2002JD002090, 2002. 6185
- Stenchikov, G., Delworth, T. L., Ramaswamy, V., Stouffer, R. J., Wittenberg, A., and Zeng, F.: Volcanic signals in oceans, *J. Geophys. Res.*, 114, D16104, doi:10.1029/2008JD011673, 2009. 6195, 6196, 6217
- Stenke, A., Schraner, M., Rozanov, E., Egorova, T., Luo, B., and Peter, T.: The SOCOL version 3.0 chemistry–climate model: description, evaluation, and implications from an advanced transport algorithm, *Geosci. Model Dev.*, 6, 1407–1427, doi:10.5194/gmd-6-1407-2013, 2013. 6186
- Toohey, M., Krüger, K., Niemeier, U., and Timmreck, C.: The influence of eruption season on the global aerosol evolution and radiative impact of tropical volcanic eruptions, *Atmos. Chem. Phys.*, 11, 12351–12367, doi:10.5194/acp-11-12351-2011, 2011. 6202
- Valcke, S.: The OASIS3 coupler: a European climate modelling community software, *Geosci. Model Dev.*, 6, 373–388, doi:10.5194/gmd-6-373-2013, 2013. 6186
- Varma, V., Prange, M., Lamy, F., Merkel, U., and Schulz, M.: Solar-forced shifts of the Southern Hemisphere Westerlies during the Holocene, *Clim. Past*, 7, 339–347, doi:10.5194/cp-7-339-2011, 2011. 6185
- Varma, V., Prange, M., Spanghehl, T., Lamy, F., Cubasch, U., and Schulz, M.: Impact of solar-induced stratospheric ozone decline on Southern Hemisphere westerlies during the Late Maunder Minimum, *Geophys. Res. Lett.*, 39, 20704, doi:10.1029/2012GL053403, 2012. 6185
- Wagner, S. and Zorita, E.: The influence of volcanic, solar and CO₂ forcing on the temperatures in the Dalton Minimum (1790–1830): a model study, *Clim. Dynam.*, 25, 205–218, 2005. 6185, 6197
- Wegmann, M., Brönnimann, S., Bhend, J., Franke, J., Folini, D., Wild, M., and Luterbacher, J.: Volcanic influence on European summer precipitation through monsoons: possible cause for “years without a summer”, *J. Climate*, submitted, 2013. 6199
- Wolf, R.: Abstract of his latest results, *Mon. Not. R. Astron. Soc.*, 21, 77–78, 1861. 6182

Sun and volcanoes: effect on the troposphere in the DM

J. G. Anet et al.

[Title Page](#)

[Abstract](#)

[Introduction](#)

[Conclusions](#)

[References](#)

[Tables](#)

[Figures](#)

[⏪](#)

[⏩](#)

[◀](#)

[▶](#)

[Back](#)

[Close](#)

[Full Screen / Esc](#)

[Printer-friendly Version](#)

[Interactive Discussion](#)

Table 1. Stratospheric aerosol optical depths at 550 nm derived from volcanic aerosol simulations Arfeuille et al. (2013) using ice core measurements from Gao et al. (2008).

Year	Aerosol optical depth		Volcano	confirmed/tentative attrib.
	NH	SH		
1794	0.02	0.04	Unknown	SH, no large eruption recorded
1796	0.12	0.02	Unknown	NH, no large eruption recorded
1809	0.12	0.42	Unknown	Tropics, eruption in Feb
1815	0.24	0.68	Tambora	8° S, Indonesia, 10 Apr
1831	0.22	0.06	Babuyan Claro	19.5° N, Philipp., date?
1835	0.36	0.23	Cosiguina	13° N, Nicaragua, 20 Jan

Sun and volcanoes: effect on the troposphere in the DM

J. G. Anet et al.

[Title Page](#)

[Abstract](#)

[Introduction](#)

[Conclusions](#)

[References](#)

[Tables](#)

[Figures](#)

[⏪](#)

[⏩](#)

[◀](#)

[▶](#)

[Back](#)

[Close](#)

[Full Screen / Esc](#)

[Printer-friendly Version](#)

[Interactive Discussion](#)

Table 2. Dalton minimum experiments: “const” denotes constant 1780 conditions. “bckgrd” denotes background aerosol emissions and volcanic emissions off. “trans” denotes transient forcing. “Ioniz.” stands for the parametrization for SPE, LEE and GCR.

Experiment name	Process			
	ΔI ($\lambda < 250$ nm)	ΔI ($\lambda > 250$ nm)	Δ Ioniz.	Δ SAD
CTRL1780	const	const	const	bckgrd
ALL	trans	trans	trans	trans
TD	trans	const	const	bckgrd
BU	const	trans	const	bckgrd
EPP	const	const	trans	bckgrd
VOLC	const	const	const	trans

Sun and volcanoes: effect on the troposphere in the DM

J. G. Anet et al.

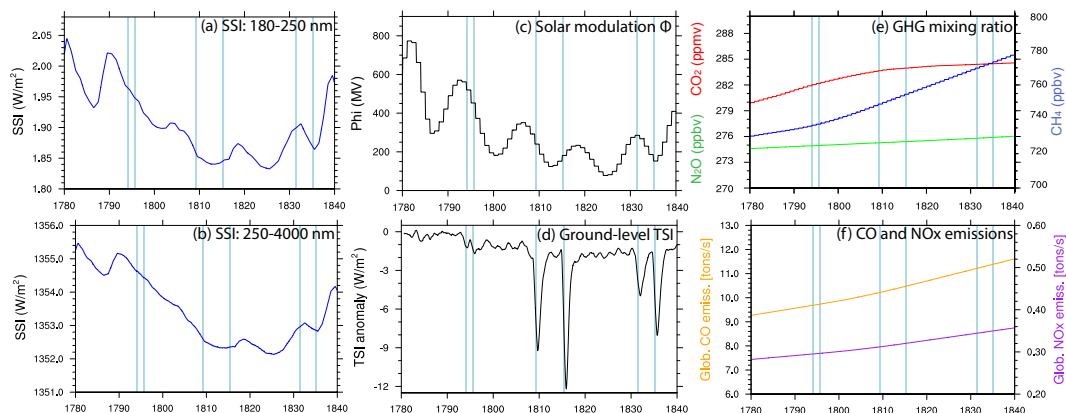


Fig. 1. Model forcing data over the Dalton Minimum (1780–1840 AD). **(a)** Spectral solar irradiance in the UV-C at $180 \text{ nm} < \lambda < 250 \text{ nm}$. **(b)** Spectral solar irradiance at $\lambda > 250 \text{ nm}$. **(c)** Solar modulation potential following Steinhilber et al. (2008). **(d)** Ground-level TSI, showing anomalies relative to the 1780 unperturbed values. **(e)** Greenhouse gas mixing ratios for CO_2 , CH_4 and N_2O . **(f)** Anthropogenic and natural CO and NO_x emissions from fossil fuel burning. Blue vertical lines highlight the years, at which a volcanic eruption occurred.

[Title Page](#)
[Abstract](#)
[Introduction](#)
[Conclusions](#)
[References](#)
[Tables](#)
[Figures](#)
[Back](#)
[Close](#)
[Full Screen / Esc](#)
[Printer-friendly Version](#)
[Interactive Discussion](#)

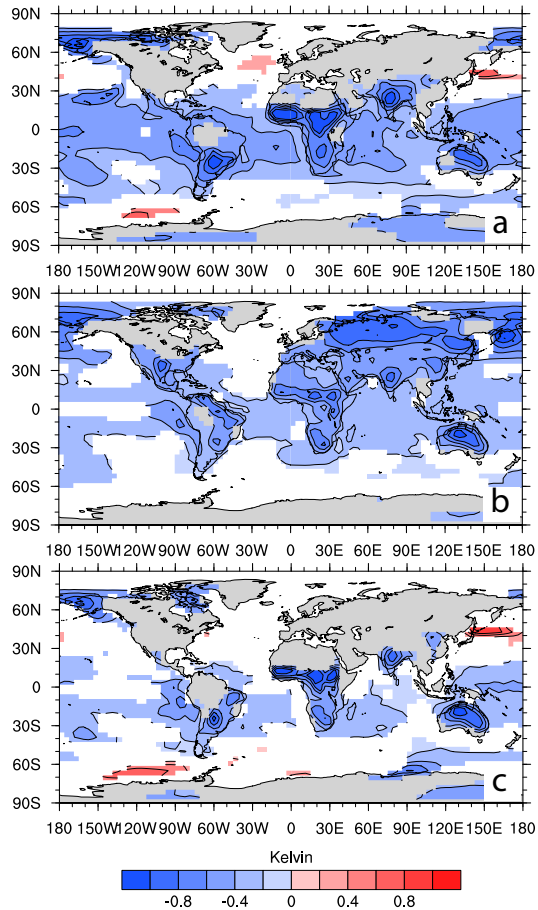


Fig. 2. (a) Ensemble mean of 2 m-temperature differences, averaged over the 1805–1825 period for the ALL run. (b) Same for the “Bottom-Up” run. (c) Same for the VOLC run. Only areas which are significant at the 5% level are colored (two sided t test).

Sun and volcanoes: effect on the troposphere in the DM

J. G. Anet et al.

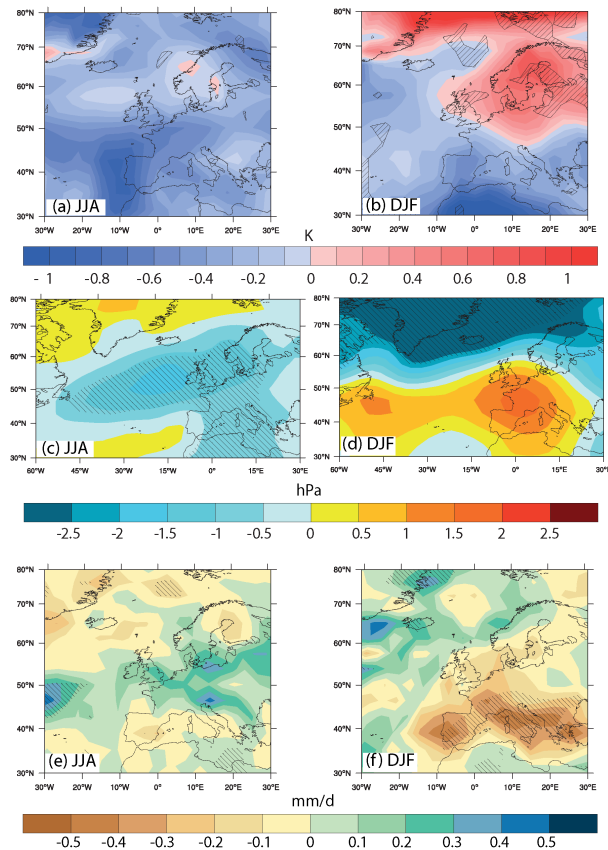


Fig. 3. Ensemble mean of post-volcanic surface temperature (**a, b**), sea level pressure (**c, d**) and precipitation (**e, f**) anomalies, showing the difference between VOLC (4 yr: 1810, 1816, 1832 and 1836) and CTRL1780 (60 yr) in the JJA (left panels) and DJF (right panels) season. For all plots, dashed areas show significant changes on a 10 % t test (two sided t test).

Sun and volcanoes: effect on the troposphere in the DM

J. G. Anet et al.

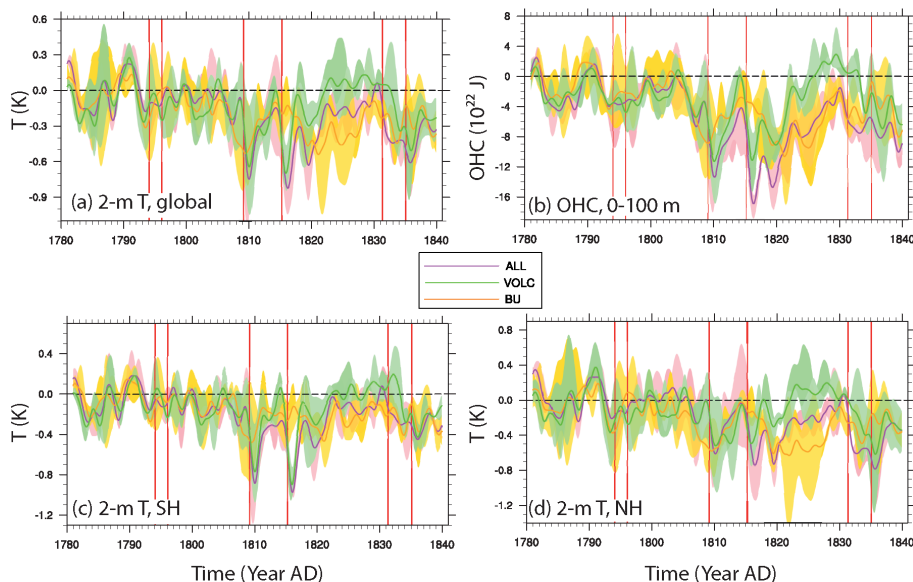


Fig. 4. Ensemble means of detrended anomalies of experiments ALL, VOLC and BU relative to CTRL1780 for **(a)** global 2 m temperatures; **(b)** global ocean heat content (OHC) of the upper ocean (first 100 m of depth); **(c)** SH 2 m temperatures; **(d)** NH 2 m temperatures. For all experiments, the envelope shows the min/max values. Red vertical lines highlight the years, at which a volcanic eruption occurred.

Sun and volcanoes: effect on the troposphere in the DM

J. G. Anet et al.

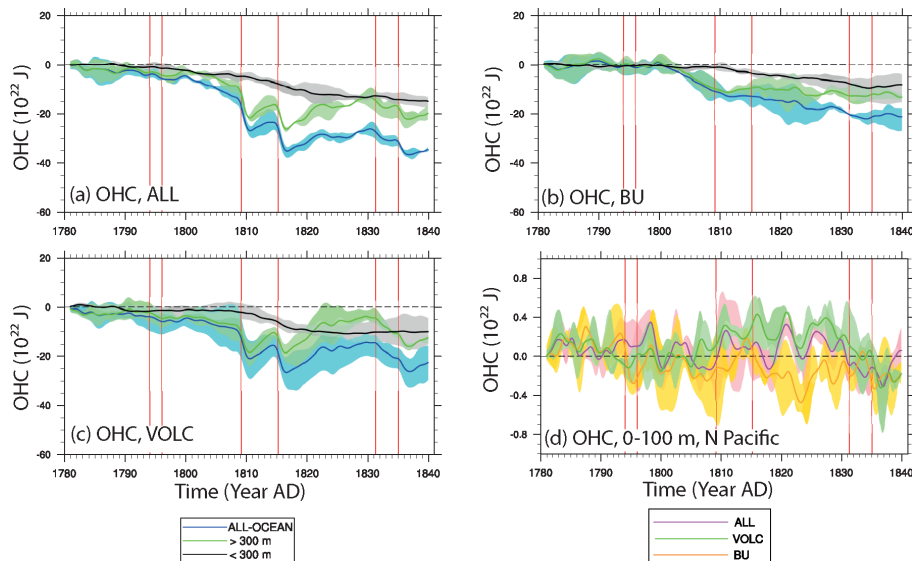


Fig. 5. Ensemble mean of detrended global ocean heat content (OHC) anomalies relative to CTRL1780, plotting technique analogue to Stenchikov et al. (2009). For **(a)–(c)**: black curve shows global total OHC (0–6020 m), green curve global OHC of the top 300 m, blue curve global OHC of the layers below 300 m (300–6020 m). **(a)** For ALL; **(b)** BU; **(c)** VOLC. **(d)** Ensemble mean of local OHC anomalies relative to CTRL1780 for the layers between 0 and 100 m of depth for the northern Pacific, Bering Sea region. Envelope shows the min/max values. Red vertical lines highlight the years, at which a volcanic eruption occurred.

[Title Page](#)
[Abstract](#)
[Introduction](#)
[Conclusions](#)
[References](#)
[Tables](#)
[Figures](#)
[Back](#)
[Close](#)
[Full Screen / Esc](#)
[Printer-friendly Version](#)
[Interactive Discussion](#)

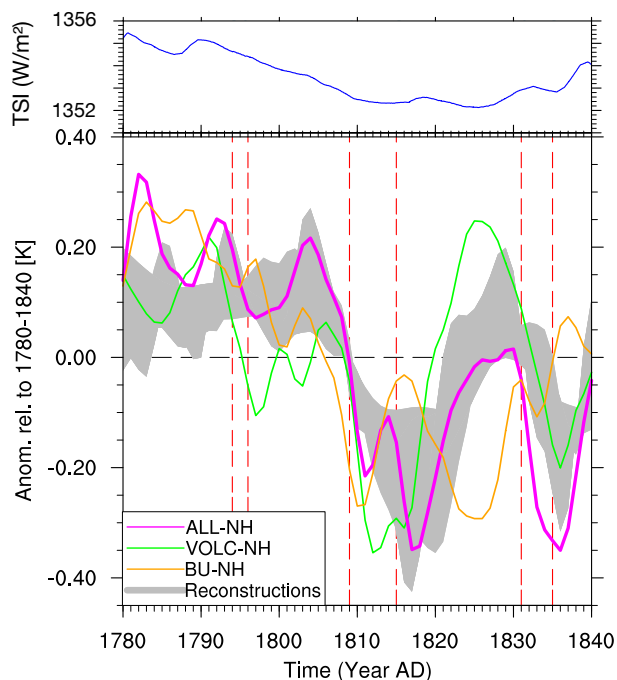


Fig. 6. Top panel: total solar irradiance from the Shapiro et al. (2011) forcing. Lower panel: model comparison with five NH temperature reconstructions of the IPCC AR4 (averaged). Magenta, green and orange lines are model curves, the grey envelope the composite of a range of tree-ring-based reconstructions. Magenta thick: ensemble mean of NH temperatures (ALL-NH). Green: same, but for the VOLC experiment (VOLC-NH). Orange: same, but for the BU experiment (BU-NH). Grey region: envelope of the five NH temperature reconstructions plotted in Fig. S2 in the Supplement. Smoothing of the model results: Gaussian 3 yr FWHM, centered on year 1. Red vertical, dashed lines highlight the years, at which a volcanic eruption occurred.

**Sun and volcanoes:
effect on the
troposphere in the
DM**

J. G. Anet et al.

[Title Page](#)

[Abstract](#) [Introduction](#)

[Conclusions](#) [References](#)

[Tables](#) [Figures](#)

[⏪](#) [⏩](#)

[◀](#) [▶](#)

[Back](#) [Close](#)

[Full Screen / Esc](#)

[Printer-friendly Version](#)

[Interactive Discussion](#)



Sun and volcanoes: effect on the troposphere in the DM

J. G. Anet et al.

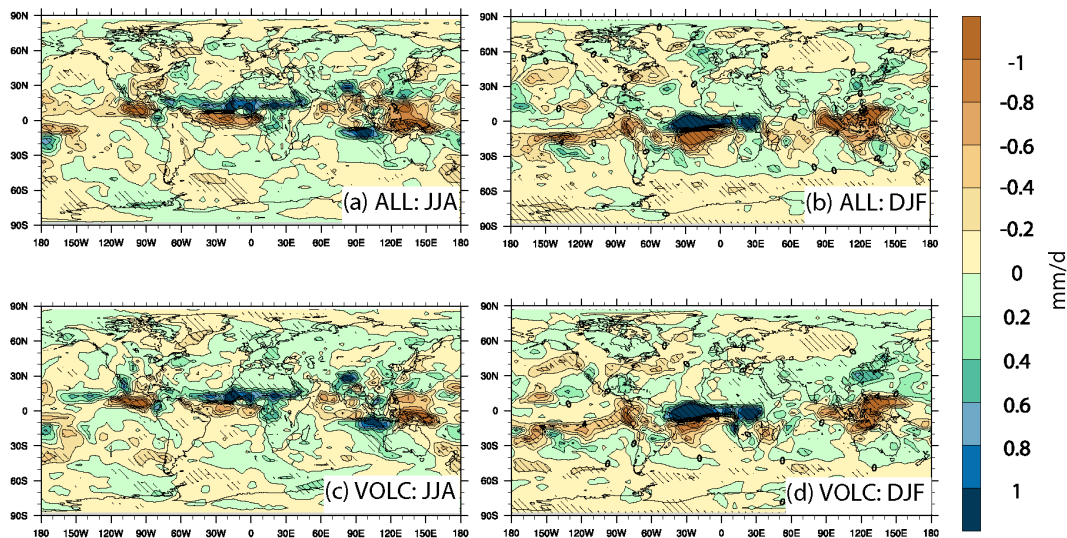


Fig. 7. (a) Ensemble mean of precipitation anomalies, averaged over the 1805–1825 period for the ALL run, JJA season. (b) Same for DJF season. (c) Same for the VOLC run, JJA season. (d) Same for the VOLC run, DJF season. For all plots, dashed areas show significant changes on a 10% t test.

[Title Page](#)

[Abstract](#)

[Introduction](#)

[Conclusions](#)

[References](#)

[Tables](#)

[Figures](#)

[⏪](#)

[⏩](#)

[◀](#)

[▶](#)

[Back](#)

[Close](#)

[Full Screen / Esc](#)

[Printer-friendly Version](#)

[Interactive Discussion](#)

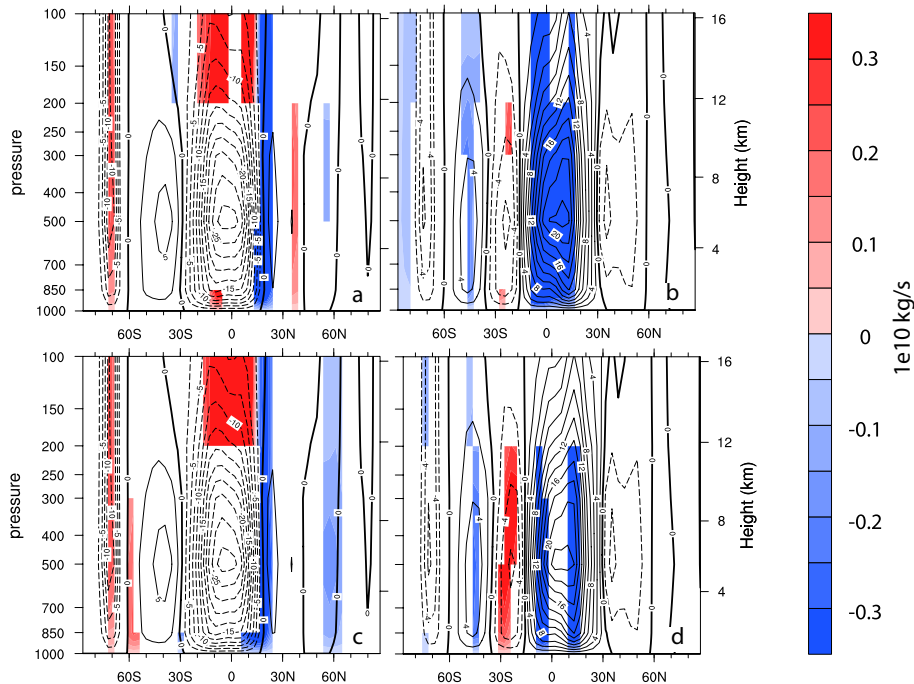


Fig. 8. (a) Ensemble mean of mass stream function anomalies, averaged over the 1805–1825 period for the ALL run, JJA season. (b) Same for the DJF season. (c) Same, but for the VOLC run, JJA season. (d) Same, but for the VOLC run, DJF season. For all plots, coloured areas show significant changes on a 10 % t test. Black contour lines show the climatology for the two seasons.

Sun and volcanoes:
effect on the
troposphere in the
DM

J. G. Anet et al.

Title Page

Abstract

Introduction

Conclusions

References

Tables

Figures

⏪

⏩

◀

▶

Back

Close

Full Screen / Esc

Printer-friendly Version

Interactive Discussion

